# Effect of miR-29a-3p in exosomes on glioma cells by regulating the PI3K/AKT/HIF-1α pathway

ZEQIANG LIU[1], ZHENG YANG[2] and LU HE[1]

[1]Department of Laboratory Medicine, Peking University Third Hospital, Beijing 100191;
[2]Department of Neurosurgery, The First People's Hospital of Jiashan, Jiaxing, Zhejiang 314100, P.R. China

Received August 10, 2022; Accepted January 16, 2023

DOI: 10.3892/mmr.2023.12959

**Abstract.** Exosomes secreted by glioma cells can carry a number of bioactive molecules. As the most abundant noncoding RNA in exosomes, microRNAs (miRNAs) are involved in signaling between tumor cells in a number of ways. In addition, hypoxia is an important feature of the microenvironment of most tumors. The present study investigated the effect of miR-29a-3p in glioma exosomes on the proliferation and apoptosis levels of U251 glioma cells under hypoxia. Qualitative PCR results showed that the expression level of miR-29a-3p in plasma exosomes of glioma patients was lower than that of normal subjects. By conducting hypoxia experiments *in vitro* on U251 glioma cells, it was found that the expression level of miR-29a-3p decreased following hypoxia, while overexpression of miR-29a-3p significantly decreased the proliferation of U251 glioma cells and promoted apoptosis by inhibiting the expression of the antiapoptotic marker Bcl-2 and increasing the expression of the proapoptotic marker Bax The potential targets of miR-29a-3p were predicted by online tools and validated by a dual-luciferase gene reporter assay. miR-29a-3p was found to target and regulate PI3K, which in turn inhibited the activity of the PI3K-AKT pathway, thereby reducing the expression of hypoxia inducible factor (HIF)-1α protein. Furthermore, the effects of miR-29a-3p on proliferation and apoptosis in glioma cells in those processes could be reversed by the PI3K-AKT agonist Recilisib. In addition, the inhibitory effect of miR-29a-3p on the PI3K/AKT/HIF-1α regulatory axis could cause a decrease in the expression levels of pyruvate dehydrogenase kinase-1 and pyruvate dehydrogenase kinase-2 and eventually lead to a reduction in glycolysis in U251 glioma cells. Similarly, Recilisib slowed the inhibitory effect of miR-29a-3p on glycolysis and glycolysis-related molecules. The results of this study tentatively confirm that miR-29a-3p carried by exosomes can be used as a novel diagnostic marker and a potential inhibitory molecule for glioma cells, providing a new theoretical and experimental basis for the precise clinical treatment of glioma.

*Correspondence to:* Dr Zeqiang Liu, Department of Laboratory Medicine, Peking University Third Hospital, 49 Huayuan North Road, Beijing 100191, P.R. China
E-mail: kku6666@hotmail.com

*Key words:* glioma, exosome, microRNA 29a-3p, hypoxia inducible factor 1α

## Introduction

Glioma is the commonest primary malignancy of the central nervous system. Despite the current combination of surgical and pharmacological treatment options for glioma, the global incidence of glioma remains high and most patients are already at a very malignant stage at the time of presentation, with a 5-year survival rate of <10% and some patients have a survival period of <2 years (1) therefore, it is crucial to explore the pathological mechanisms of glioma to find more effective treatments for the disease.

The malignant proliferation of glioma cells is often accompanied by a hypoxic growth environment due to inadequate blood vessel formation and a severe lack of oxygen supply within the tissue (2). Hypoxia affects several aspects of glioma cells, including invasion, proliferation, heterogeneity and drug resistance (2-4). Hypoxia-inducible factor-1α (HIF-1α) is a molecule closely related to hypoxia that can accumulate in the cytoplasm under hypoxia and subsequently enter the nucleus to regulate the expression of molecules closely related to the hypoxic response through the hypoxia response element, thus affecting the formation of neovascularization, cell metabolism and apoptosis in tumors under hypoxia (2-5). Since the growth environment of glioma is in hypoxia, exploring the growth characteristics of glioma under hypoxia cannot be separated from the role of hypoxia-related molecules (e.g., HIF-1α). Studying the relationship between them may provide a possible way for early diagnosis and treatment of glioma cells.

In addition, a number of lipids microvesicles of 30-100 nm in diameter, called exosomes, have been found in the blood of some glioma patients (2-6). These exosomes can isolate and extract a variety of small RNAs, proteins, lipids and other substances as signaling molecules for molecular transduction and cross-linking between tumor cells (7). It has been shown that microRNAs (miRNAs) isolated from exosomes are involved in the regulation of tumor cell growth, metabolism and apoptosis through various pathways and have potential value for early tumor diagnosis (8). miRNAs are a class of RNA molecules 18-22 bases in length that do not have a coding

function but can affect protein expression by inhibiting the transcription and translation process of proteins. miR-29a-3p is a molecule that is abnormally expressed in a variety of tumor cells and can regulate oncogenes in recent years (9,10). In the present study, the expression level of miR-29a-3p in plasma exosomes of patients with glioma in The First People's Hospital of Jiashan (China) was examined and the effects of miR-29a-3p on the proliferation and apoptosis of glioma cells under hypoxia were verified by cell experiments. Then, the mechanism of the effect of exosomes and their included miRNAs on glioma was explored. The present study may provide a possible theoretical basis for the early diagnosis and targeted therapy of glioma.

Table I. Clinical characteristics of glioma patients.

| Grouping information | Characteristic |
|---|---|
| Sample size | n=20 |
| Sex | 8 males and 12 females |
| Age (years) | 55.85±10.16 |
| Tumor classification | WHO I-II grade (n=9) |
| | WHO III-IV grade (n=11) |

WHO, World Health Organization.

## Materials and methods

*Sample collection*. Peripheral blood (~10 ml) was collected from 20 patients with glioma who underwent routine surgery in the Department of Neurosurgery and 20 healthy controls in the Health Management Centre between January 2019 and December 2020 at The First People's Hospital of Jiashan. The patients and healthy controls consisted of 8 males and 12 females, respectively, aged 42-68 years, the clinicopathological features of patients are presented in Table I.

The inclusion criteria were i) Glioma confirmed by postoperative pathology, ii) no preoperative radiotherapy or chemotherapy was given, iii) first time of brain tumor resection and iv) patients with complete clinical records. Exclusion criteria were i) previous history of brain surgery, ii) combination with other tumor diseases, mental diseases and other encephalopathy affecting neurological function and iii) complications with serious heart, liver and kidney diseases. All patients had pathological confirmation of glioma and had not been previously treated with chemotherapy. All subjects were formally informed of the purpose of sample use and signed the informed consent form. The present study was approved by the Ethics Committee of Jiashan First People's Hospital (approval no. KY2022-030).

*Reagents*. Human glioma U251 cells were purchased from Shanghai CAS Cell Bank, DMEM was purchased from Gibco (Thermo Fisher Scientific, Inc.), fetal bovine serum, TRIzol®, One Step PrimeScript cDNA Synthesis kit, Lipofectamine® 2000 were purchased from Thermo Fisher Scientific, Inc., trypsin-EDTA solutions (0.25%) were purchased from MilliporeSigma, a plasma exosome extraction kit was purchased from Invitrogen (Thermo Fisher Scientific, Inc.), a qPCR kit was purchased from Takara Bio USA, Inc. The miR-29-3p-5p mimic/inhibitor was synthesized by Shanghai Jima Co., Ltd., the double luciferase gene reporter assay was commissioned from Tianjin Sheweisi Biotechnology Co., Ltd., the CCK-8 cell viability assay kit was purchased from Bestbio, Annexin V-phycoerythrin (PE) and 7-AAD were purchased from Becton, Dickinson and Company, rabbit anti-human PI3K (cat. no. 4249), AKT (cat. no. 4685) and phosphorylated (p-)AKT (cat. no. 4060) antibodies were purchased from Cell Signaling Technology, Inc., rabbit anti-human HIF-1α (cat. no. 20960-1-AP) antibodies were purchased from Proteintech Group, Inc. and rabbit anti-human Bax (cat. no. 41162) antibody was purchased from Cell Signaling Technology, Inc., rabbit anti-human Bcl-2 (cat. no. ab32124), pyruvate dehydrogenase kinase (PDK)-1 (cat. no. ab202468), PDK2 (cat. no. ab154549) from Abcam, β-actin (cat. no. TA-09), goat anti-rabbit secondary antibody (cat. no. ZB-5301) was purchased from Beijing Zhongshan Jinqiao Biotechnology Co., Ltd., the PVDF membrane was purchased from MilliporeSigma (cat. no. ISEQ00010), the ECL luminescent solution was purchased from Jiangsu KGI Biotechnology Co., Ltd. (cat. no. KGP1127) and the glycolysis assay kit was purchased from Agilent (cat. no. 103020-100).

*Isolation and identification of exosomes*. The plasma sample was centrifuged at room temperature (25˚C) for 20 min at 2,000 x g; the supernatant was transferred to a new centrifuge tube and centrifuged at 4˚C for 30 min at 2,000 x g; the supernatant was transferred to a new precooled centrifuge tube and centrifuged again at 4˚C for 45 min at 10,000 x g to remove the larger vesicles. The supernatant was collected by filtration through a 0.45 $\mu$m membrane and centrifuged at 4˚C for 70 min at 100,000 x g. The supernatant was removed, resuspended in 10 ml of precooled 1x PBS, and centrifuged again at 4˚C for 70 min at 100,000 x g. The supernatant was removed and the resulting precipitate was the exosome. In addition, the exosome information was analyzed using the ExoCarta database (http://www.exocarta.org; version 3.1.4).

*Transmission electron microscopy (TEM)*. For TEM 10 $\mu$l exosomes were placed onto copper-coated grids and precipitated for 10 min and the excess liquid was absorbed by filter paper. The grids were transferred to a solution containing 2.5% glutaraldehyde (diluted with PBS) at 4˚C, suspended for 5 min and dried with filter paper before being washed with PBS for four times. The grids were transferred to 40 g/l uranyl acetate (MilliporeSigma) for 10 min at 25˚C and the excess liquid was absorbed by filter paper. The grids were transferred to 10 g/l methyl-cellulose (MilliporeSigma) for 5 min at 25˚C and dried with filter paper. After natural drying at room temperature (25˚C; ~30 min), the grids were analyzed on a HT-7700 transmission electron microscope (Hitachi, Ltd.) and images were analyzed by Digital Micrograph (version 3.51, Gatan, Inc.).

*Cell culture and drug treatment*. The human glioma cell line U251 was cultured using DMEM complete medium containing 10% fetal bovine serum. The normal culture conditions were 5% $CO_2$ + 95% air in a constant temperature incubator at 37˚C; the hypoxic culture conditions were 5% $CO_2$ + 94% $N_2$ + 1%

Table II. miR-29a-3p mimics/inhibitor/control and PI3K/β-actin primer sequences.

| Gene | Primer sequence |
|---|---|
| miR-29a-3p mimics | F: 5'-UAGCACCAUCUGAAAUCGGUUA-3' |
| | R: 5'-ACCGAUUUCAGAUGGUGCUAUU-3' |
| Mimics control | F: 5'-UUCUCCGAACGUGUCACGUTT-3' |
| | R: 5'-ACGUGACACGUUCGGAGAATT-3' |
| miR-29a-3p inhibitor | F: 5'-UAACCGAUUUCAGAUGGUGCUA-3' |
| Inhibitor control | R: 5'-CAGUACUUUUGUGUAGUACAA-3' |
| PI3K | F: 5'-GGACCCGATGCGGTTAGAG-3' |
| | R: 5'-ATCAAGTGGATGCCCCACAG-3' |
| β-actin | F: 5'-GTGGATCAGCAAGCAGGAGT-3" |
| | R: 5'-CTCGGCCACATTGTGAACTT-3' |

miR, microRNA; F, forward; R, reverse.

$O_2$ and the cells were placed in a hypoxic incubator at 37˚C. Recilisib complete medium with a masterbatch concentration of 100 mM was prepared and cells were transfected for 24 h and incubated at 37˚C, then added to the cell supernatant at 1:1,000 and mixed as the miR-29a-3p + Recilisib group. The miR-NC + DMOG group was used as the control group to start the experiment 48 h after transfection.

*Transfection of miR-29a-3p mimics and inhibitor.* Glioma cells in the log growth phase were selected and inoculated in 6-well plates at a rate of $2x10^5$ cells/well and the transfection experiment was started when the cell confluence reached 60%. During transfection, 12 $\mu$l Lipofectamine® 2000 was added to 150 $\mu$l serum-free medium and mixed with 10 $\mu$l miR-29a-3p mimics/inhibitors, then incubated at room temperature (25˚C). The final concentration of miR-29a-3p mimics was 50 nM and the final concentration of miR-29a-3p inhibitor was 100 nM. After incubation for 5 min, the mixed solution was added to the 6-well plates to complete the transfection. The miR-29a-3p control group (miR-NC) received the same processing. After 48 h, the transfection efficiency of each well was measured by reverse transcription-quantitative (RT-q) PCR. The sequences of the miR-29a-3p mimics/inhibitor/control are given in Table II.

*RT-qPCR.* The cells were spread into 6-well plates at $2x10^5$ cells/well, 1 ml TRIzol® (Thermo Fisher Scientific, Inc.) was added when the convergence degree of the cells was 80-90% and total RNA was extracted by the TRIzol® method. For mRNA, cDNA was formed by reverse transcription according to the instructions of the One Step PrimeScript cDNA Synthesis kit (Thermo Fisher Scientific, Inc.) and mir-X miRNA first-strand synthesis kit (Takara Biotechnology Co., Ltd.) was used for miRNA. RT-qPCR R was performed using TB Green® Advantage® qPCR premix regent (Takara Biotechnology Co., Ltd.) and the results were calculated by the $2^{-\Delta\Delta Cq}$ method to detect the relative expression of the genes (11), using U6 as the internal reference for miRNA and β-actin as the internal reference for mRNA. The reaction conditions were as follows: 95˚C, 2 min, followed by 40 cycles of 10 sec at 95˚C, 30 sec at 55˚C and 30 sec at 72˚C. The primer sequences (purchased from Sangon Biotech, Shanghai) are given in Table II.

*Cell proliferation assay.* Cell proliferation was detected by the CCK-8 assay. Cells were seeded into 96-well plates at $2x10^4$ cells/well and complete medium without cells was used as a blank control. After the cells were grown for 24 h, 10 $\mu$l of CCK-8 solution was added to each well and ~3-5 replicate wells were set up in each well. The cells were cultured in an incubator for 2.5 h at 37˚C and the D450 value was measured at 450 nm with a microplate reader. Cell proliferation level=(experimental group-blank group)/(untreated group-blank group) x100%.

*Apoptosis detected by flow cytometry.* Cells ($2.5x10^6$ cells/tube) were collected, centrifuged at 4˚C for 5 min at 210 x g and washed 3 times with precooled PBS. Then cells were collected again, centrifuged at 4˚C for 5 min at 160 x g and suspended with 100 $\mu$l 1X binding buffer. Annexin V-PE (5 $\mu$l) was added and cells were incubated at 4˚C for 15 min containing after which 7-AAD was added and incubated for 5 min at 4˚C. Annexin V-PE was used to detect early apoptotic cells, and Annexin V-PE and 7-AAD were used to detect necrotic cells or/and late apoptotic cells. The percentage of early apoptotic cells was used to calculate the apoptotic rate and the cell apoptosis level was detected by a BD Accuri C6 Flow cytometer and analyzed by BD Accuri C6 Software (version 1.0; BD Biosciences).

*Dual-Luciferase reporter assay.* The binding site of miR-29-3p-5p to PI3K was predicted by the online database Targets can (https://www.targetscan.org/vert_80/; version 8.0). Wild-type PI3K 3'-UTR (WT-PI3K) or mutant PI3K 3'-UTR (MUT-PI3K) was inserted into the *Xho*I and *Not*I sites of the pSI-Check2 vector (Sangon Biotech Co., Ltd.), respectively. Plasmid transfection was performed when the cell density reached ~50-70%. Briefly, 5 pmol miR-29 mimics or miR-29 control was mixed with 0.16 $\mu$g PI3K 3'-UTR (WT-UTR) plasmid or PI3K 3'-UTR (MUT-PI3K) plasmid, respectively, then above solution were mixed with 10 $\mu$l DMEM containing 0.3 $\mu$l Lipofectamine® 2000 (Thermo Fisher Scientific, Inc.) and placed at room temperature (25˚C) for 20 min before transfection. Following transfection, the transfected cells were incubated in the incubator for 48 h at 37˚C, then cells were

collected. Passive Lysis Buffer was added at 100 µl/well at room temperature (25˚C) and slowly shaken for 15 min, then the cell lysate was aspirated into a 1.5 ml centrifuge tube, centrifuged at 4˚C at 13,000 x g for 10 min and the supernatant was taken and transferred into a new tube. Luciferase Assay Agent II (LAR II; 100 µl; Promega Corporation) and 20 µl cell lysate were added. The firefly luciferase value (R1) was measured by Promega Dual Luciferase system (Promega Corporation) after 2 sec. Then, 100 µl Stop & Glo reagent (Luciferase Assay Reagent; Promega Corporation) was added and mixed 2-3 times and the Renilla luciferase value of each well (R2) was detected. Finally, the ratio value (R1/R2) was recorded as the relative luciferase activity.

*Western blotting*. The cells were lysed in RIPA buffer: 50 mM Tris-HCl (MilliporeSigma), 150 mM NaCl (MilliporeSigma), 1% Triton X(MilliporeSigma), 1% Sodium deoxycholate (MilliporeSigma), 0.1% SDS (MilliporeSigma), 5 mM EDTA (MilliporeSigma), with 2 µg/ml aprotinin (MilliporeSigma), 1 mmol/l PMSF (Beijing Solarbio Science & Technology Co., Ltd.), and the protein concentration was measured by the BCA method. After protein extraction, 50 µg of proteins were loaded per lane and 10% of SDS-PAGE gels were prepared to separate the proteins, which were then transferred to PVDF membranes. Skimmed milk powder (5%) was used for blocking for 2 h at room temperature and the membranes incubated with primary antibodies against PI3K (1:2,000), AKT (1:1,000), p-AKT (1:1,000), Bax (1:1,000), Bcl-2 (1:1,000), HIF-1α (1:2,000), PDK-1 (1:1,000), PDK-2 (1:1,000) and β-actin (1:4,000) overnight at 4˚C. This was followed by incubation with a secondary antibody (1:5,000) for 2 h at room temperature, color development with ECL luminescent solution and the protein levels were measured using a ChemiDoc MP Imaging System (Bio-Rad Laboratories, Inc.). Image Lab 5.1 (Bio-Rad Laboratories, Inc.) was used to analyze the gray values.

*Glycolytic capacity was examined with a Seahorse system*. The cells were inoculated at $1.5x10^5$ cells/well into energy metabolism assay plates. A total of five secondary wells were set up for each strain of cells and the plates were soaked with activation solution and placed in a $CO_2$-free incubator at 37˚C overnight. On the second day, 1 ml of sodium pyruvate was added to 100 ml of XF Base medium and the pH was adjusted to 7.35-7.45. The prepared XF base medium was used to wash the cells twice and 500 µl of XF base medium was added and placed in the cell culture box for 1 h. Oligomycin, 2-DG and glucose working solutions were prepared and added to the dosing wells of the hydration plate. The hydration plate was moved to the machine and programmed according to the Energy Metabolizer manual XFe24 Training Manual (Seahorse Bioscience; Agilent Technologies, Inc.). After 1 h of running the program, the cell culture plate was placed on the machine and after 2 h, the glycolysis level of the cells was analyzed.

*Statistical analysis*. All data are expressed as the mean ± standard deviation. A t-test was used for intragroup comparisons and one-way ANOVA was used for comparisons between multiple groups. $P<0.05$ was considered to indicate a statistically significant difference.

## Results

*miR-29a-3p expression levels in plasma exosomes of patients with glioma*. The purified exosomes were examined using TEM, as shown in Fig. 1A, where unevenly distributed vesicle-like structures <200 nm in diameter with a lipid bilayer structure can be seen against a dark background and were more typical. The particle size analysis revealed that the particle size value was 76.64±13.25 nm and diameters between 30-150 nm accounted for >90% of all vesicles (Fig. 1B), indicating that the vesicles obtained were of uniform diameter and high purity. Then the expression of miR-29a-3p was detected. In plasma exosomes of patients with glioma, the miRNA-29a-3p levels were evaluated by RT-qPCR. The results showed a significant decrease in miR-29a-3p expression levels in plasma exosomes from glioma patients compared with those from healthy controls (Fig. 1C).

*Effect of miR-29a-3p on proliferation and apoptosis levels in gliomas under normoxic and hypoxic conditions*. The expression levels of miR-29a-3p in the glioma cell line U251 were examined by RT-qPCR. The results showed that the expression levels of miR-29a-3p in glioma cells were decreased under hypoxic conditions (Fig. 2A) compared with normoxia. In addition, it was found that hypoxia increased the proliferation level of glioma cells, but overexpression of miR-29a-3p significantly inhibited their proliferation (Fig. 2B). The results of flow cytometry showed that overexpression of miR-29a-3p significantly increased apoptosis in glioma cells under normoxic and hypoxic conditions (Fig. 2C). Western blotting was applied to examine apoptosis-related proteins. Overexpression of miR-29a-3p increased the pro-apoptotic marker Bax while decreasing the anti-apoptotic marker Bcl-2. The role of miR-29a-3p in the above processes was more prominent under normoxic conditions. In addition, glioma cells under normoxic conditions expressed a certain level of hypoxia-Inducible Factor (HIF)-1 and hypoxia increased its expression, whereas the overexpression of miR-29-3p inhibited its expression (Fig. 2D).

*miR-29a-3p inhibits HIF-1α expression by targeting the PI3K/AKT pathway*. TargetScan was used to predict the presence of miR-29a-3p binding sites in the PI3K gene. Then to further understand the target role of miR-29a-3p on PI3K, dual-luciferase gene reporter assay was performed. Results showed that in Wt-PI3K groups, compared with miR-NC, miR-29a-3p mimics could decrease the luciferase activity. However, when the binding site of PI3K to miR-29a-3p was mutated (MUT-PI3K), miR-29a-3p lost its effect on the luciferase activity, the above results indicated the target regulation of miR-29a-3p on PI3K gene (Fig. 3A and B). qPCR and western blotting results showed that miR-29a-3p could inhibit PI3K protein expression, resulting in a reduction in AKT phosphorylation levels and HIF-1α protein expression levels, as shown in Fig. 3C-E.

*Effect of miR-29a-3p on glioma proliferation and apoptosis levels through targeting the regulation of the PI3K/AKT/HIF-1α pathway*. The present study investigated the effect of miR-29a-3p on the proliferation and apoptosis of glioma cells via the PI3K/AKT/HIF-1α regulatory axis under normoxia because

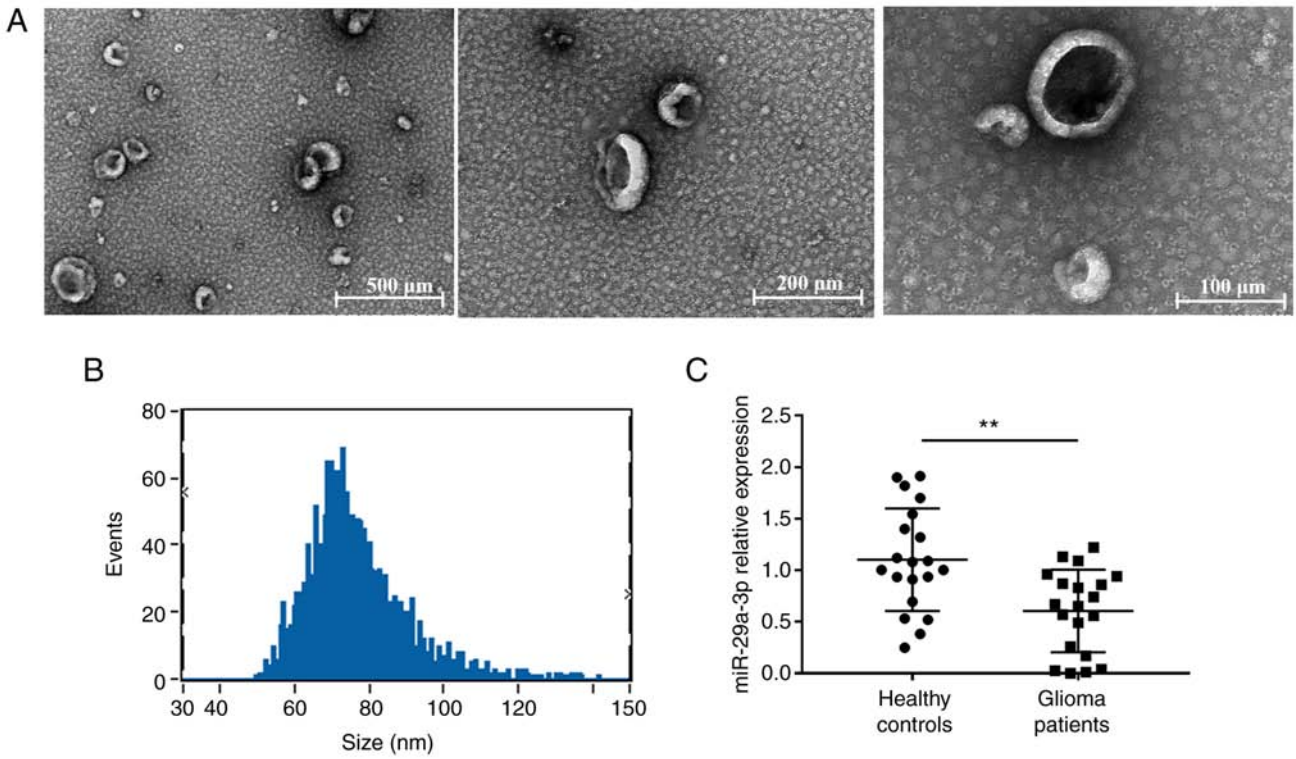


Figure 1. Plasma exosome expression of miR-29a-3p in healthy controls and glioma patients. Identification and analysis of particle size by transmission electron microscopy of peripheral blood exosomes. (A) Exosomes by transmission electron microscopy. (B) Peak diagram of exosome particle size. (C) Reverse transcription-quantitative PCR showed the expression levels of miR-29a-3p in plasma exosomes in healthy controls (n=20) and glioma patients (n=20). Data were expressed as the mean ± standard deviation and the experiment was repeated three times for each group, $^{**}$P<0.01. miR, microRNA.

HIF-1α exhibited a certain expression level under normoxia and previous experiments demonstrated that overexpression of miR-29a-3p could have a more pronounced effect on apoptosis under normoxic conditions. The results showed that overexpression of miR-29a-3p significantly reduced cell proliferation, increased apoptosis and the expression of the pro-apoptotic molecule Bax. In addition, it reduced the expression of the anti-apoptotic molecule Bcl-2 and HIF-1α, p-AKT, AKT and PI3K compared with the control group (miR-NC) after 24 h of normoxic culture. By contrast, when the PI3K agonist Recilisib was used, the inhibitory effect of miR-29a-3p on cell proliferation and apoptosis, the reduction in PI3K, AKT, p-AKT, Bcl-2 and HIF-1α expression and the increase in Bax expression levels were all reversed, as shown in Fig. 4.

*miR-29a-3p inhibits glycolysis levels in glioma cells by targeted regulation of the PI3K/AKT/HIF-1α pathway*. The results showed that compared with the control group (miR-NC, miR-NC + DMSO), overexpression of miR-29a-3p significantly inhibited the expression of HIF-1α, PDK1 and PDK2, thereby decreasing the ECAR level in glioma cells. However, when Recilisib was used (miR-29a-3p + Recilisib group), the expression levels of HIF-1α and PDK1 and PDK2 were increased and the ECAR level was enhanced compared with the miR-29a-3p overexpression group, as shown in Fig. 5A and B.

## Discussion

Normal brain cells are supplied with normal oxygen concentrations (~20%), while the oxygen concentrations in glioma cells are between 0.1-2.5% (12). Glioma cells are in a state of chronic hypoxia but do not inhibit the proliferation of tumor cells. This growth characteristic stimulates more abnormal gene expression, making them more adapted to hypoxia. Therefore, hypoxia is one of the key features of the glioma growth microenvironment (13). The search for mechanisms of malignant transformation of glioma cells under hypoxic conditions may provide alternative directions to resolve these problems.

Studies have demonstrated that hypoxia can increase the secretion of exosomes in tumor cells or cause the loss of the transportation of more molecules (14-16). Exosomes act as carriers of intercellular molecular signals and can carry a variety of oncogenes or inhibitory factors that affect the different stages of tumor growth (17,18). Research on the composition and molecular function of exosomes is of great diagnostic and clinical importance. In addition, according to the ExoCarta database, exosomes are known to contain 9,769 proteins, 3,408 mRNAs and 1,116 lipids, among which there are 2,838 types of miRNAs, accounting for the highest proportion of noncoding RNAs in exosomes (19,20). Exosomes deliver these miRNAs to other target cells and are extensively involved in tumor proliferation, apoptosis, cycling, invasion and adhesion-related processes by regulating the 3' untranslated region (UTR) of target molecules and degrading mRNA directly or indirectly (21,22). Therefore, the detection of exosomes may be of great value to the diagnosis of diseases and other research.

The exosomes derived from peripheral blood may originate from some peripheral blood cells, such as lymphocytes, monocytes and/or from tumors and other normal cells. Based

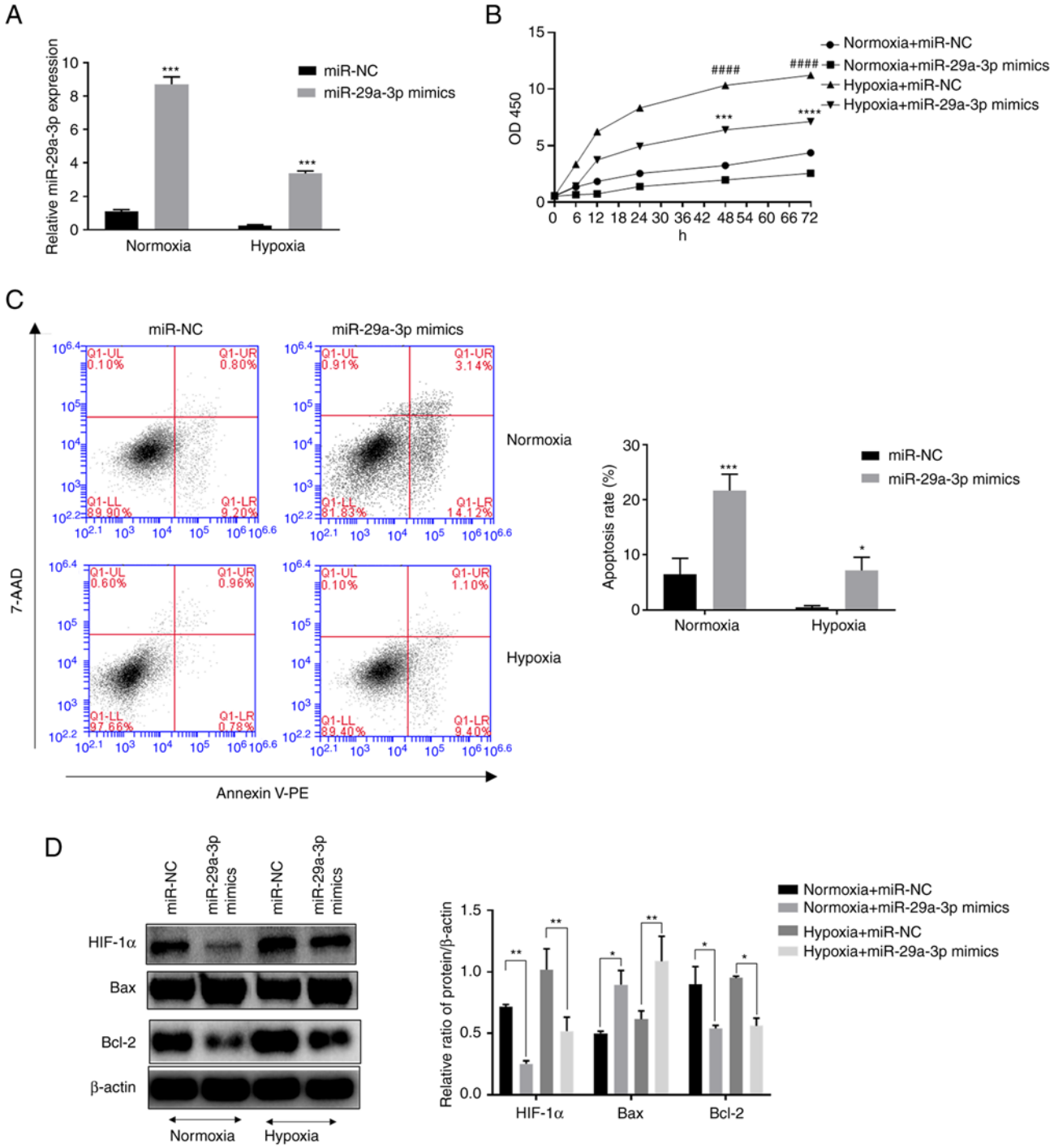


Figure 2. Effect of miR-29a-3p on the proliferation and apoptosis levels of glioma cells under normoxic and hypoxic conditions. (A) The expression level of miR-29a-3p by reverse transcription-quantitative PCR, $^{***}$P<0.001 vs. miR-NC under hypoxia. (B) The effect of miR-29a-3p on the proliferation level of glioma cells U251, $^{\#\#\#\#}$P<0.0001 vs. miR-NC under normoxia; $^{***}$P<0.001, $^{****}$P<0.0001 vs. miR-NC under hypoxia. (C) Effect of miR-29a-3p on apoptotic levels in glioma cells U251, $^{*}$P<0.05 vs. miR-NC under hypoxia, $^{***}$P<0.001 vs. miR-NC under normoxia. (D) Effect of miR-29a-3p on the expression levels of Bax, Bcl-2 and HIF-1α. $^{*}$P<0.05, $^{**}$P<0.01. All data were expressed as the mean ± standard deviation (n=3). miR, microRNA; NC, negative control; HIF-1α, hypoxia-inducible factor 1.

on the above, the substance in exosomes such as miR-29a-3p may have different significance and effects. Reports have shown that the detection of miR-29a-3p in glioma can be used as a malignant marker after making a definite diagnosis (23-25), then, if possible, the glioma can be staged according to the expression of miR-29a-3p and clinical data. As miR-29a-3p expressed in peripheral blood can be used as a biomarker for the preliminary diagnosis of disease, and may be used as an early marker for disease screening, this highlights the significance of detecting it in peripheral blood (26-29).

In addition, the miR-29a-3p-derived exosomes may originate from glioma cells and then affect the differentiation of functional peripheral blood cells, such as mediating the expansion and function of myeloid-derived suppressor cells and assisting tumors in evading the host immune response (30).

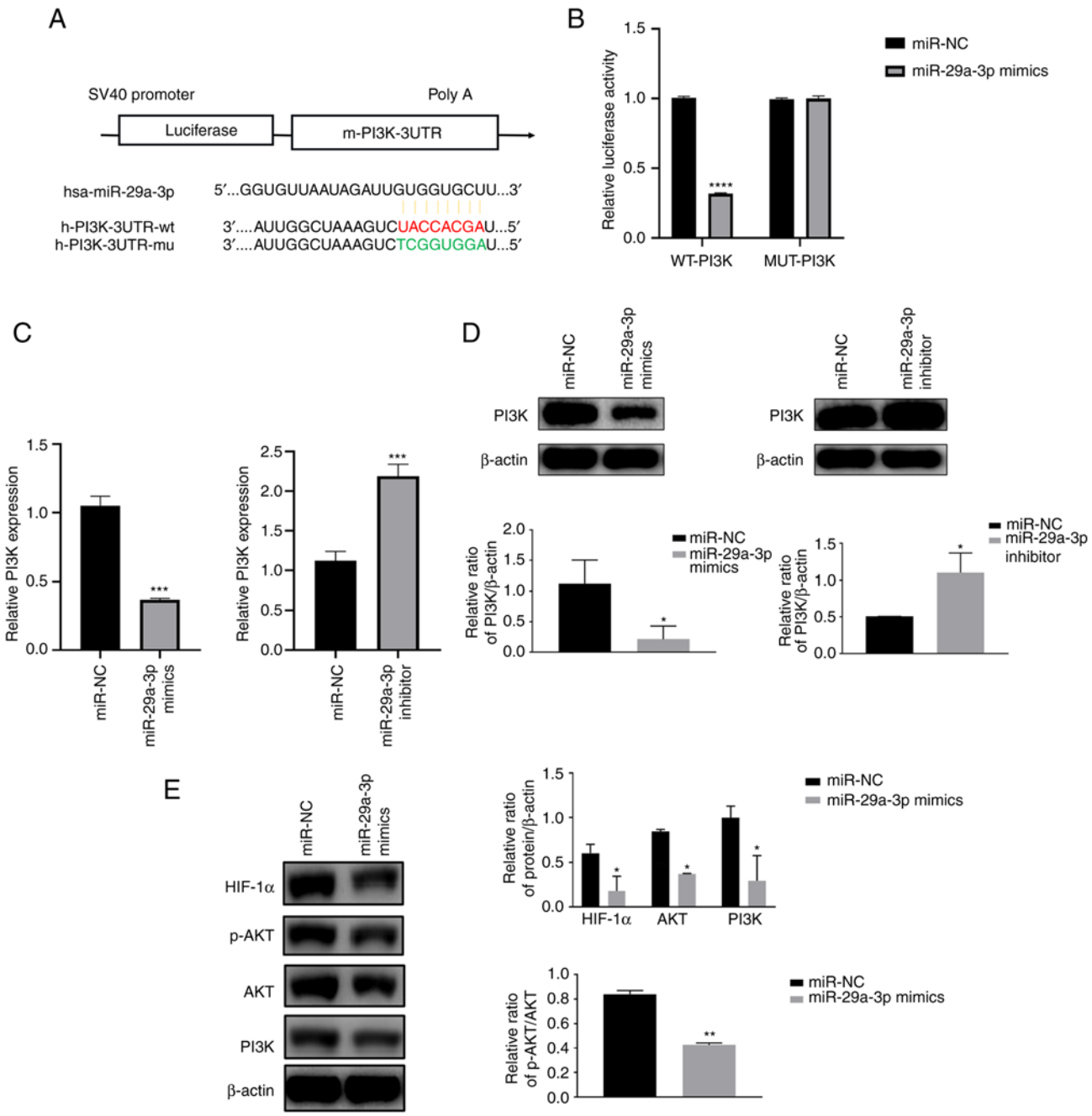


Figure 3. miR-29a-3p inhibits HIF-1α expression by targeting the PI3K/AKT pathway. (A) A schematic diagram of the binding site of miR-29a-3p to the PI3K gene and the PI3K mutation site was predicted by TargetScan. (B) Dual luciferase gene reporter assay was used to verify the targeting negative regulatory effect of miR-29a-3p on PI3K, $^{****}$P<0.0001. The expression level of PI3K was analyzed by (C) quantitative PCR and (D) western blotting after U251 cells were transfected with miR-29a-3p mimics and inhibitor, $^{*}$P<0.05, $^{***}$P<0.001. (E) Effect of miR-29a-3p on the expression levels of the PI3K downstream molecules AKT, p-AKT and HIF-1α, $^{*}$P<0.05, $^{**}$P<0.01. All data were expressed as the mean ± standard deviation (n=3). miR, microRNA; HIF-1α, hypoxia-inducible factor 1; NC, negative control; UTR, 3' untranslated region; wt, wild-type; mu, mutant; p-, phosphorylated.

However, the specific mechanism of miR-29a-3p transmitted by peripheral blood cells for glioma remains to be elucidated. In addition, how miR-29a-3p affects the glioma cells needs to be experimentally verified, which is also the purpose of the present study. The present study found that miR-29a-3p was significantly lower in plasma exosomes of glioma patients compared with normal subjects and that its expression increased apoptosis and inhibited proliferation levels of glioma cells, initially showing the cancer marker effect of miR-29a-3p.

The core response event of hypoxia is the reduction of oxygen concentration. Therefore, exploring the effects of the hypoxic microenvironment on tumor cells can be studied using molecules closely related to oxygen metabolism. In-depth studies reveal that miR-29a significantly inhibits the expression of HIF-1α, a key regulatory molecule closely associated with hypoxia (31). HIF-1α is an oxygen stress molecule that is degraded by the ubiquitin-proteasome pathway when oxygen is available. It accumulates stably in the cytoplasm when the oxygen concentration is reduced and then enters the nucleus

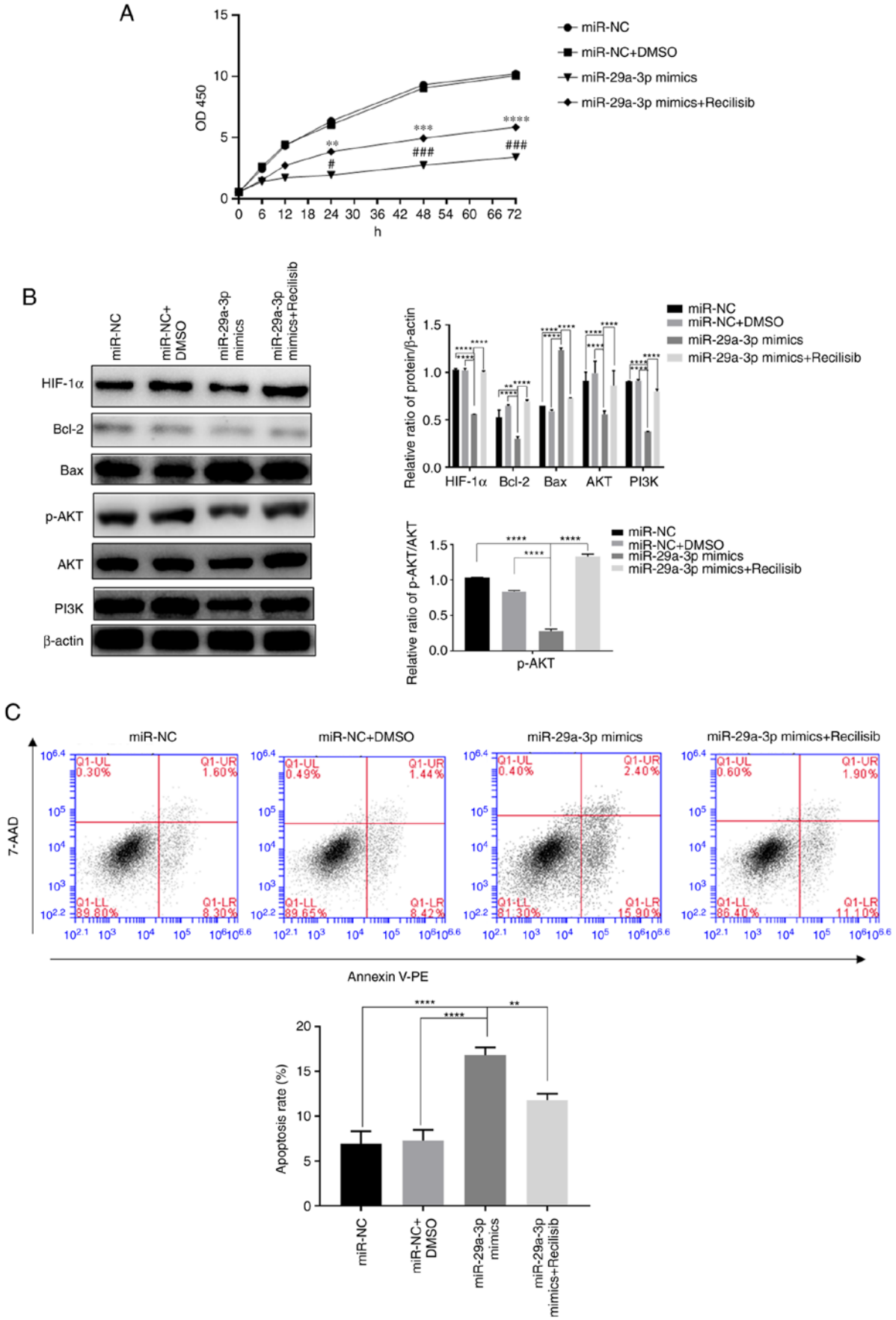


Figure 4. The effect of miR-29a-3p via the PI3K/AKT/HIF-1α pathway on glioma cells' proliferation and apoptosis levels. (A) The proliferation level was detected by CCK-8 assay, $^{**}$P<0.01, $^{***}$P<0.001, $^{****}$P<0.0001 vs. miR-NC + DMSO; $^{\#}$P<0.05, $^{\#\#\#}$P<0.001 vs. miR-NC. (B) The expression levels of HIF-1α, Bcl-2, Bax, AKT, PI3K and the ratio of p-AKT/AKT, were detected by western blotting, $^{**}$P<0.01, $^{****}$P<0.0001. (C) The levels of apoptosis in each group were detected by flow cytometry, $^{**}$P<0.01, $^{****}$P<0.0001. All data were expressed as the mean ± standard deviation (n=3). miR, microRNA; HIF-1α, hypoxia-inducible factor 1; NC, negative control; HIF-1α, hypoxia-inducible factor 1; p-, phosphorylated; PE, phycoerythrin.

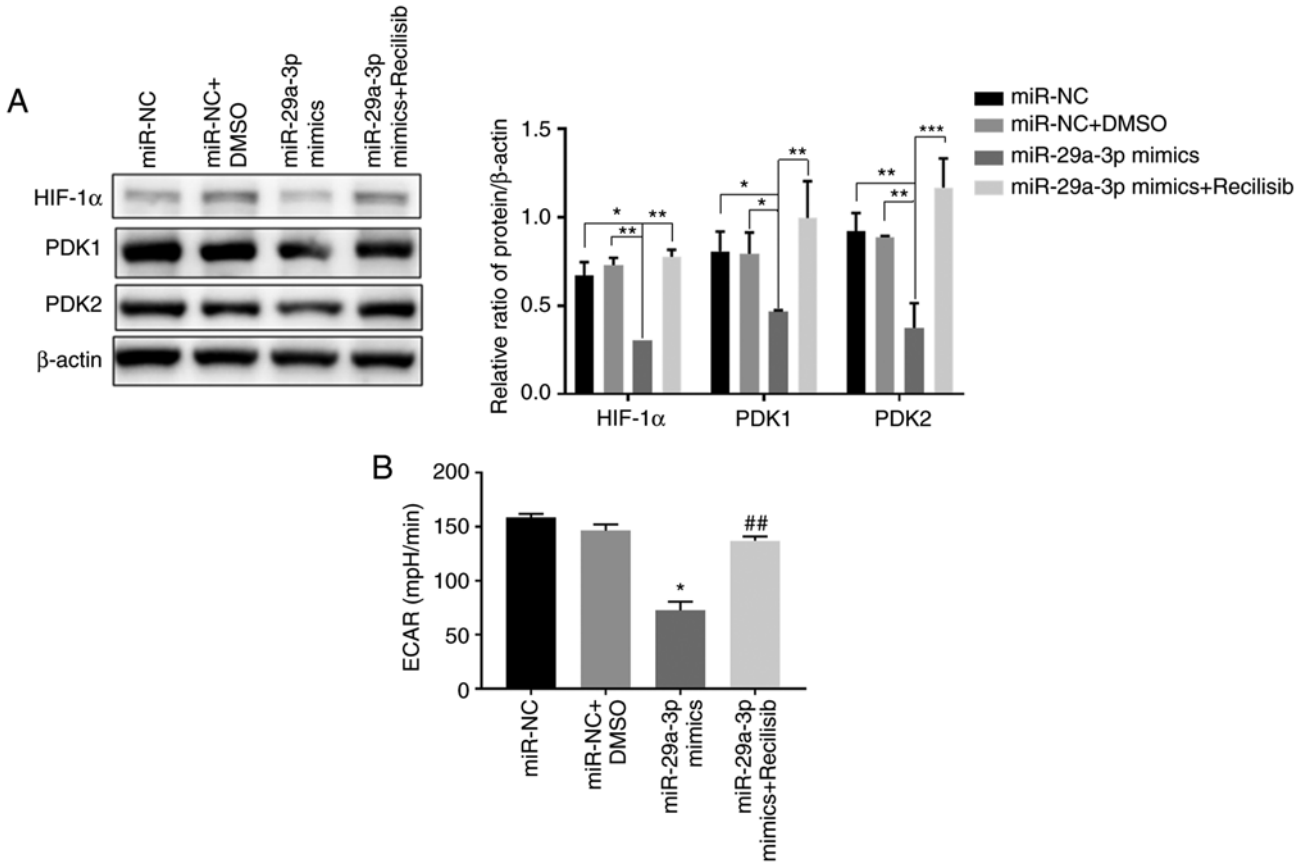


Figure 5. The effect of miR-29a-3p on glycolysis levels in glioma cells. (A) The expression levels of HIF-1α, PDK1 and PDK2 were detected by western blotting, $^{*}$P<0.05, $^{**}$P<0.01, $^{***}$P<0.001. (B) The level of glycolysis in each group was detected by Seahorse energy metabolism assay; $^{*}$P<0.05 vs. miR-NC, $^{\#\#}$P<0.01 vs. miR-29a-3p mimics. All data were expressed as the mean ± standard deviation (n=3). miR, microRNA; HIF-1α, hypoxia-inducible factor 1; PDK, pyruvate dehydrogenase kinase; NC, negative control.

to serve a transcriptional regulatory role. HIF-1α expressed in the nucleus can form a dimer with HIF-1β, that is, the complete HIF-1 protein, which can affect the survival of tumor cells in a hypoxic environment through a variety of pathways. U251 is a glioblastoma cell line with a high degree of malignancy that is in a serious hypoxic state inside the tumor tissue. To adapt to hypoxia, genes inside the tumor cells are abnormally expressed so that the expression of HIF-1α is not dependent on reduced oxygen levels (32,33), which explains why this tumor cell also has a certain level of HIF-1α protein under normoxic conditions. In addition, the present study showed that hypoxia could reduce the apoptosis level and increase the proliferation of U251 cells. Harmful metabolic intermediates in normal cells can be removed in time, while in malignant tumors with rapid growth, the metabolism of tumor cells is relatively vigorous and abnormally vigorous metabolic processes will cause cells to accumulate more products that cannot be removed promptly (34-36). A number of studies have found that the number of mitochondria in malignant tumors is less than that in surrounding normal cells; their shapes are different and they are more prone to degeneration and change (37-39). Abnormal mitochondrial function is not only deprived of the efficient use of oxygen for energy supply but also increases the production of reactive oxygen species (ROS) and harmful intermediate metabolites, the incomplete elimination of which, especially those derived from biological processes related to oxygen, may accumulate more into the cell, have adverse effects on nucleic acid, protein structure, amino acid modification, energy metabolism and other molecular biological activities and ultimately cause the onset of cell apoptosis and death (40-42). Nevertheless, for some malignancies, glycolysis has become their major source of energy and hypoxia could initially reduce the oxygen intake of cells, which can lead to lower levels of tumor oxidative phosphorylation and then reduce the accumulation of metabolic hazards related to oxygen, such as ROS, which explains why cells had improved survival under hypoxia in the present study. In addition, studies have shown that HIF-1α can inhibit the accumulation of harmful metabolites such as lactic acid and ROS through various pathways and then enhance tumor cell survival in other ways, such as increasing the expression of VEGF to promote neovascularization, increasing the expression of the antiapoptotic molecule Bcl-2 and decreasing the expression of the proapoptotic molecule Bax to inhibit tumor cell apoptosis or increasing the level of cellular glycolysis through glucose transporter/PDK to maintain tumor cell growth (43-46). Therefore, the presence of HIF-1α under normoxia can avoid the apoptosis and death of tumor cells to a certain extent, but once the expression of HIF-1α is inhibited, the tumor cells without HIF-1α compensation cannot effectively inhibit the harmful metabolites and their apoptosis will also increase, which explains why the inhibition of HIF-1α expression in

glioma cells by miR-29a-3p caused more apoptosis production compared with hypoxic conditions.

The PI3K-AKT pathway is involved in the regulation of cell proliferation, differentiation, apoptosis and glucose transport (47-50). The main biological functions of miR-29a target genes are also focused on these aspects, so there may be an association between the two. PI3K/AKT is an important antiapoptotic pathway and several molecules affected by this pathway, such as VEGF and endothelial NOS in angiogenesis, Bad, Bcl-2 and BNIP3 in apoptosis and the glioma cell invasion molecule PAI-1, are associated with the expression of HIF-1α, which is an important molecule regulated by the PI3K/AKT pathway upon activation (51,52). Therefore, it is reasonable to hypothesize that the process of HIF-1α inhibition by miR-29a-3p may occur via the PI3K/AKT pathway and this phenomenon was confirmed in the present experiments. In addition, the Warburg effect is the use of glycolysis by tumor cells under normoxia as their main metabolic mode of energy production (53,54). By contrast, HIF-1α can regulate the level of glycolysis by promoting the transcriptional activation of pyruvate dehydrogenase kinase (PDK), a key rate-limiting enzyme of glycolysis, thereby inhibiting pyruvate dehydrogenase activity and thus preventing pyruvate from participating in the tricarboxylic acid cycle instead of participating in the glycolytic pathway (55). This change in the energy metabolism of glioma cells is an important reason for tumor heterogeneity, aggressiveness and increased drug resistance. The results of the present study showed that the overexpression of miR-29a-3p could significantly inhibit the expression of PDK1 and PDK2, which in turn caused a decrease in the glycolysis level of glioma cells. By contrast, the activation of the PI3K pathway using Recilisib based on overexpression of miR-29a-3p could partially restore the glycolysis level of tumor cells. The above results revealed that miR-29a-3p inhibited glycolysis in tumor cells through the PI3K/AKT/HIF-1α pathway, thus affecting the proliferation and apoptosis levels of glioma cells.

The present study had several limitations. First, the experiments were performed in only one glioma cell line, more glioma cell lines should be applied to validate the experimental consequence in future research. Second, cell proliferation and apoptosis should need more methods based on molecular biology approaches to further verify the experimental results.

Currently, the main treatment option for glioma patients is surgical resection combined with radiotherapy. However, the limitations of surgical resection, drug resistance and resistance to radiotherapy have resulted in short survival cycles, high mortality and recurrence rates. As a result, a number of researchers are focusing on early diagnosis and molecularly targeted therapy for patients with glioma. The results of the present study revealed that miR-29a-3p is an important suppressor molecule in glioma and this molecule can inhibit the growth and proliferation of glioma cells by targeting the negative regulation of the PI3K/AKT/HIF-1α pathway and reducing glycolytic energy supply, thus increasing the apoptosis of glioma cells. The present study reveals the potential value of miR-29a-3p in tumor diagnosis and treatment and provides an additional theoretical basis for the screening of novel molecular markers for glioma and possible therapeutic pathways.

**Acknowledgements**

Not applicable.

**Funding**

The present study was partially supported by 'Research on comprehensive prevention and control technology, accurate risk assessment and application demonstration of individualized prevention and control measures for senile prostate hyperplasia', National Key R&D projects (grant no. 2021YFC2009300).

**Availability of data and materials**

The datasets generated and/or analyzed during the current study are not publicly available due to information that could compromise the privacy of research participants but are available from the corresponding author upon reasonable request.

**Authors' contributions**

ZL was responsible for data acquisition, experimental design, analysis and interpretation and drafting of the article, including primer design, result statistics, charting. LH conceptualized and co-designed the study, critically screened the revised article for important intellectual content and provided final approval of the submitted manuscript. ZY was responsible for sample acquisition. ZL and ZY confirm the authenticity of all the raw data. All authors have read and approved the final manuscript.

**Ethics approval and consent to participate**

The protocol for this assay was approved by the Ethics Committee of Jiashan First People's Hospital (approval no. KY2022-030). Subjects provided written informed consent to participate in this study.

**Patient consent for publication**

Not applicable.

**Competing interests**

The authors declare that they have no competing interests.

**References**

1. Touati S, Djekkoun R, El-Okki ME and Satta D: Epidemiology and survival analyses of 333 adult glioma patients from Eastern Algeria (2008-2016). Afr Health Sci 20: 1250-1258, 2020.
2. Domènech M, Hernández A, Plaja A, Martínez-Balibrea E and Balañà C: Hypoxia: The cornerstone of glioblastoma. Int J Mol Sc 22: 12608, 2021.
3. Mohlin S, Wigerup C, Jögi A and Påhlman S: Hypoxia, pseudohypoxia and cellular differentiation. Exp Cell Res 356: 192-196, 2017.
4. Tamai S, Ichinose T, Tsutsui T, Tanaka S, Garaeva F, Sabit H and Nakada M: Tumor microenvironment in glioma invasion. Brain Sci 12: 505, 2022.
5. Ke Q and Costa M: Hypoxia-inducible factor-1 (HIF-1). Mol Pharmacol 70: 1469-1480, 2006.
6. Saadatpour L, Fadaee E, Fadaei S, Nassiri Mansour R, Mohammadi M, Mousavi SM, Goodarzi M, Verdi J and Mirzaei H: Glioblastoma: Exosome and microRNA as novel diagnosis biomarkers. Cancer Gene Ther 23: 415-418, 2016.

7. Whiteside TL: Tumor-derived exosomes and their role in cancer progression. Adv Clin Chem 74: 103-141, 2016.
8. Yu X, Odenthal M and Fries JWU: Exosomes as miRNA carriers: Formation-function-future. Int J Mol Sci 17: 2028, 2016.
9. Wang JY, Zhang Q, Wang DD, Yan W, Sha HH, Zhao JH, Yang SJ, Zhang HD, Hou JC, Xu HZ, *et al*: MiR-29a: A potential therapeutic target and promising biomarker in tumors. Biosci Rep 38: BSR20171265, 2018.
10. Yan B, Guo Q, Fu FJ, Wang Z, Yin Z, Wei YB and Yang JR: The role of miR-29b in cancer: Regulation, function, and signaling. Onco Targets Ther 8: 539-548, 2015.
11. Livak KJ and Schmittgen TD: Analysis of relative gene expression data using real-time quantitative PCR and the 2(-Delta Delta C(T)) method. Methods 25: 402-408, 2021.
12. Yahara K, Ohguri T, Udono H, Yamamoto J, Tomura K, Onoda T, Imada H, Nishizawa S and Korogi Y: Radiotherapy using IMRT boosts after hyperbaric oxygen therapy with chemotherapy for glioblastoma. J Radiat Res 58: 351-356, 2017.
13. Zhang S, Luo X, Wan F and Lei T: The roles of hypoxia-inducible factors in regulating neural stem cells migration to glioma stem cells and determinating their fates. Neurochem Res 37: 2659-2666, 2012.
14. Cheng H, Chang S, Xu R, Chen L, Song X, Wu J, Qian J, Zou Y and Ma J: Hypoxia-challenged MSC-derived exosomes deliver miR-210 to attenuate post-infarction cardiac apoptosis. Stem Cell Res Ther 11: 224, 2020.
15. Jiang H, Zhao H, Zhang M, He Y, Li X, Xu Y and Liu X: Hypoxia induced changes of exosome cargo and subsequent biological effects. Front Immunol 13: 824188, 2022.
16. Sun H, Meng Q, Shi C, Yang H, Li X, Wu S, Familiari G, Relucenti M, Aschner M, Wang X and Chen R: Hypoxia-inducible exosomes facilitate liver-tropic premetastatic niche in colorectal cancer. Hepatology 74: 2633-2651, 2021.
17. Kumar A and Deep G: Exosomes in hypoxia-induced remodeling of the tumor microenvironment. Cancer Lett 488: 1-8, 2020.
18. Yaghoubi S, Najminejad H, Dabaghian M, Karimi MH, Abdollahpour-Alitappeh M, Rad F, Mahi-Birjand M, Mohammadi S, Mohseni F, Sobhani Lari M, *et al*: How hypoxia regulate exosomes in ischemic diseases and cancer microenvironment? IUBMB Life 72: 1286-1305, 2020.
19. Sheehan C and D'Souza-Schorey C: Tumor-derived extracellular vesicles: Molecular parcels that enable regulation of the immune response in cancer. J Cell Sci 132: jcs235085, 2019.
20. Indira Chandran V, Welinder C, Gonçalves de Oliveira K, Cerezo-Magaña M, Månsson AS, Johansson MC, Marko-Varga G and Belting M: Global extracellular vesicle proteomic signature defines U87-MG glioma cell hypoxic status with potential implications for non-invasive diagnostics. J Neurooncol 144: 477-488, 2019.
21. van der Vos KE, Abels ER, Zhang X, Lai C, Carrizosa E, Oakley D, Prabhakar S, Mardini O, Crommentuijn MH, Skog J, *et al*: Directly visualized glioblastoma-derived extracellular vesicles transfer RNA to microglia/macrophages in the brain. Neuro Oncol 18: 58-69, 2016.
22. Cai Q, Zhu A and Gong L: Exosomes of glioma cells deliver miR-148a to promote proliferation and metastasis of glioblastoma via targeting CADM1. Bull Cancer 105: 643-651, 2018.
23. He PY, Yip WK, Chai BL, Chai BY, Jabar MF, Dusa N, Mohtarrudin N and Seow HF: Inhibition of cell migration and invasion by miR-29a-3p in a colorectal cancer cell line through suppression of CDC42BPA mRNA expression. Oncol Rep 38: 3554-3566, 2017.
24. Wang J, Chen X, Xie C, Sun M, Hu C, Zhang Z, Luan L, Zhou J, Zhou J, Zhu X, *et al*: MicroRNA miR-29a inhibits colon cancer progression by downregulating B7-H3 expression: Potential molecular targets for colon cancer therapy. Mol Biotechnol 63: 849-861, 2021.
25. Kuo TY, Hsi E, Yang IP, Tsai PC, Wang JY and Juo SHH: Computational analysis of mRNA expression profiles identifies microRNA-29a/c as predictor of colorectal cancer early recurrence. PLoS One 7: e31587, 2012.
26. Yamada A, Horimatsu T, Okugawa Y, Nishida N, Honjo H, Ida H, Kou T, Kusaka T, Sasaki Y, Yagi M, *et al*: Serum miR-21, miR-29a, and miR-125b are promising biomarkers for the early detection of colorectal neoplasia. Clin Cancer Res 21: 4234-4242, 2015.
27. Uratani R, Toiyama Y, Kitajima T, Kawamura M, Hiro J, Kobayashi M, Tanaka K, Inoue Y, Mohri Y, Mori T, *et al*: Diagnostic potential of cell-free and exosomal MicroRNAs in the identification of patients with high-risk colorectal adenomas. PLoS One 11: e0160722, 2016.
28. Marcuello M, Duran-Sanchon S, Moreno L, Lozano JJ, Bujanda L, Castells A and Gironella M: Analysis of A 6-Mirna signature in serum from colorectal cancer screening participants as non-invasive biomarkers for advanced adenoma and colorectal cancer detection. Cancers (Basel) 11: 1542, 2019.
29. Huang Z, Huang D, Ni S, Peng Z, Sheng W and Du X: Plasma microRNAs are promising novel biomarkers for early detection of colorectal cancer. Int J Cancer 127: 118-126, 2010.
30. Guo X, Qiu W, Wang J, Liu Q, Qian M, Wang S, Zhang Z, Gao X, Chen Z, Guo Q, *et al*: Glioma exosomes mediate the expansion and function of myeloid-derived suppressor cells through microRNA-29a/Hbp1 and microRNA-92a/Prkar1a pathways. Int J Cancer 144: 3111-3126, 2019.
31. Huang YH, Lian WS, Wang FS, Wang PW, Lin HY, Tsai MC and Yang YL: MiR-29a curbs hepatocellular carcinoma incidence via targeting of HIF-1α and ANGPT2. Int J Mol Sci 23: 1636, 2022.
32. Agani F and Jiang BH: Oxygen-independent regulation of HIF-1: Novel involvement of PI3K/AKT/mTOR pathway in cancer. Curr Cancer Drug Targets 13: 245-251, 2013.
33. Wang J, Chen X, Hu H, Yao M, Song Y, Yang A, Xu X, Zhang N, Gao J and Liu B: PCAT-1 facilitates breast cancer progression via binding to RACK1 and enhancing oxygen-independent stability of HIF-1α. Mol Ther Nucleic Acids 24: 310-324, 2021.
34. Currie E, Schulze A, Zechner R, Walther TC and Farese RV Jr: Cellular fatty acid metabolism and cancer. Cell Metab 18: 153-161, 2013.
35. Tang Y, Xiao G, Shen Z, Zhuang C, Xie Y, Zhang X, Yang Z, Guan J, Shen Y, Chen Y, *et al*: Noninvasive detection of extracellular pH in human benign and malignant liver tumors using CEST MRI. Front Oncol 10: 578985, 2020.
36. Xu L, Wang L, Zhou L, Dorfman RG, Pan Y, Tang D, Wang Y, Yin Y, Jiang C, Zou X, *et al*: The SIRT2/cMYC pathway inhibits peroxidation-related apoptosis in cholangiocarcinoma through metabolic reprogramming. Neoplasia 21: 429-441, 2019.
37. Zong WX, Rabinowitz JD and White E: Mitochondria and cancer. Mol Cell 61: 667-676, 2016.
38. Guerra F, Arbini AA and Moro L: Mitochondria and cancer chemoresistance. Biochim Biophys Acta Bioenerg 1858: 686-699, 2017.
39. Porporato PE, Filigheddu N, Pedro JMB, Kroemer G and Galluzzi L: Mitochondrial metabolism and cancer. Cell Res 28: 265-280, 2018.
40. Księżakowska-Łakoma K, Żyła M and Wilczyński JR: Mitochondrial dysfunction in cancer. Prz Menopauzalny 13: 136-144, 2014.
41. Beltrà M, Pin F, Ballarò R, Costelli P and Penna F: Mitochondrial dysfunction in cancer cachexia: Impact on muscle health and regeneration. Cells 10: 3150, 2021.
42. Hsu CC, Tseng LM and Lee HC: Role of mitochondrial dysfunction in cancer progression. Exp Biol Med (Maywood) 241: 1281-1295, 2016.
43. Liu ZZ, Tian YF, Wu H, Ouyang SY and Kuang WL: LncRNA H19 promotes glioma angiogenesis through miR-138/HIF-1α/VEGF axis. Neoplasma 67: 111-118, 2020.
44. Miska J, Lee-Chang C, Rashidi A, Muroski ME, Chang AL, Lopez-Rosas A, Zhang P, Panek WK, Cordero A, Han Y, *et al*: HIF-1α Is a metabolic switch between glycolytic-driven migration and oxidative phosphorylation-driven immunosuppression of tregs in glioblastoma. Cell Rep 27: 226-237.e4, 2019.
45. Wang Z, Li Q, Xia L, Li X, Sun C, Wang Q, Cai X and Yang G: Borneol promotes apoptosis of human glioma cells through regulating HIF-1a expression via mTORC1/eIF4E pathway. J Cancer 11: 4810-4822, 2020.
46. Gabriely G, Wheeler MA, Takenaka MC and Quintana FJ: Role of AHR and HIF-1α in glioblastoma metabolism. Trends Endocrinol Metab 28: 428-436, 2017.
47. Yang D, Fan L, Song Z, Fang S, Huang M and Chen P: The KMT1A/TIMP3/PI3K/AKT circuit regulates tumor growth in cervical cancer. Reprod Biol 22: 100644, 2022.
48. Ma Y, Ran D, Zhao H, Song R, Zou H, Gu J, Yuan Y, Bian J, Zhu J and Liu Z: Cadmium exposure triggers osteoporosis in duck via P2X7/PI3K/AKT-mediated osteoblast and osteoclast differentiation. Sci Total Environ 750: 141638, 2021.
49. Zhang W, Hou J, Yan X, Leng J, Li R, Zhang J, Xing J, Chen C, Wang Z and Li W: Platycodon grandiflorum saponins ameliorate cisplatin-induced acute nephrotoxicity through the NF-κB-mediated inflammation and PI3K/Akt/apoptosis signaling pathways. Nutrients 10: 1328, 2018.

50. Iheagwam FN, Iheagwam OT, Onuoha MK, Ogunlana OO and Chinedu SN: Terminalia catappa aqueous leaf extract reverses insulin resistance, improves glucose transport and activates PI3K/AKT signalling in high fat/streptozotocin-induced diabetic rats. Sci Rep 12: 10711, 2022.
51. Zhang Z, Yao L, Yang J, Wang Z and Du G: PI3K/Akt and HIF-1 signaling pathway in hypoxia-ischemia (review). Mol Med Rep 18: 3547-3554, 2018.
52. Zheng HL, Wang LH, Sun BS, Li Y, Yang JY and Wu CF: Oligomer procyanidins (F2) repress HIF-1α expression in human U87 glioma cells by inhibiting the EGFR/AKT/mTOR and MAPK/ERK1/2 signaling pathways in vitro and in vivo. Oncotarget 8: 85252-85262, 2017.
53. D'Alessandro G, Quaglio D, Monaco L, Lauro C, Ghirga F, Ingallina C, De Martino M, Fucile S, Porzia A, Di Castro MA, *et al*: $^{1}$H-NMR metabolomics reveals the glabrescione B exacerbation of glycolytic metabolism beside the cell growth inhibitory effect in glioma. Cell Commun Signal 17: 108, 2019.
54. Mao XG, Xue XY, Wang L, Wang L, Li L and Zhang X: Hypoxia regulated gene network in glioblastoma has special algebraic topology structures and revealed communications involving Warburg effect and immune regulation. Cell Mol Neurobiol 39: 1093-1114, 2019.
55. Kim JW, Tchernyshyov I, Semenza GL and Dang CV: HIF-1-mediated expression of pyruvate dehydrogenase kinase: A metabolic switch required for cellular adaptation to hypoxia. Cell Metab 3: 177-185, 2006.